POLITECNICO DI TORINO
Repository ISTITUZIONALE

Interactions between motor unit firing and fascicle dynamics during shortening and lengthening contractions

Original
Interactions between motor unit firing and fascicle dynamics during shortening and lengthening contractions / Arvanitidis, M., Pincheira, P.A., Negro, F., Botter, A., Cerone, G.L., Martinez-Valdes, E.. - In: JOURNAL OF NEUROPHYSIOLOGY. - ISSN 0022-3077. - STAMPA. - 136:2(2026), pp. 735-744. [10.1152/jn.00188.2026]

Availability:
This version is available at: 11583/3017243 since: 2026-11-04T08:40:59Z

Publisher:
APS

Published
DOI:10.1152/jn.00188.2026

Terms of use:

This article is made available under terms and conditions as specified in the corresponding bibliographic description in the repository

Publisher copyright

(Article begins on next page)

18 November 2026

american physiological society | JNP JOURNAL OF NEUROPHYSIOLOGY

J Neurophysiol 136: 735–744, 2026.
First published July 22, 2026; doi:10.1152/jn.00188.2026

SHORT REPORT

Control of Movement

Interactions between motor unit firing and fascicle dynamics during shortening and lengthening contractions

Michail Arvanitidis,[1] Patricio A. Pincheira,[2,3,4] Francesco Negro,[5] Alberto Botter,[6] Giacinto Luigi Cerone,[6] and Eduardo Martinez-Valdes[1]

[1]*Centre of Precision Rehabilitation for Spinal Pain, School of Sport, Exercise and Rehabilitation Sciences, University of Birmingham, Birmingham, United Kingdom;* [2]*School of Health, Medical and Psychological Sciences, University of Southern Queensland, Ipswich, Queensland, Australia;* [3]*School of Human Movement and Nutrition Sciences, The University of Queensland, Brisbane, Queensland, Australia;* [4]*Centre for Innovation in Pain and Health Research, School of Health & Rehabilitation Sciences, The University of Queensland, Brisbane, Queensland, Australia;* [5]*Department of Clinical and Experimental Sciences, Università degli Studi di Brescia, Brescia, Italy; and* [6]*Laboratory for Engineering of the Neuromuscular System (LISiN) and PoliToBIOMed Laboratory, Department of Electronics and Telecommunications, Politecnico di Torino, Turin, Italy*

Abstract

The integration of high-density surface electromyography with ultrasound-transparent electrodes (HDsEMG-US) and B-mode ultrasonography enables concurrent assessment of motor unit (MU) firing properties and fascicle length (FL) from the same muscle region. Although the isometric relations between MU discharge, FL, and torque have been characterized, their interactions during anisometric contractions remain poorly understood. This study examined MU discharge behavior and its relation with FL changes during shortening and lengthening contractions of the tibialis anterior muscle. Ten healthy males performed isokinetic dorsiflexion contractions at a constant angular velocity of 2°/s while maintaining a constant submaximal torque of 25% maximum voluntary contraction torque, measured at a long muscle-tendon length (∼30° of plantarflexion), with HDsEMG-US signals and ultrasound images recorded simultaneously. MUs were identified using blind-source separation decomposition and FL was tracked with an optical flow algorithm. Cross-correlation analysis revealed high associations between cumulative spike train (CST), FL, and torque in both contraction phases. Neuromechanical delays were significantly longer during lengthening than shortening (phase effect: $F_{1,7} = 8.51$, $P = 0.023$; mean difference: −25.04 ms, 95% CI: −45.35 to −4.74). Discharge rate changed at a similar rate with variations in FL during both shortening and lengthening contractions (similar discharge rate-FL slopes, $P = 0.44$); however, absolute discharge rates were systematically lower during lengthening (difference in intercepts: $P < 0.0001$). These findings demonstrate the feasibility of HDsEMG-US for characterizing neuromechanical coupling during dynamic contractions and provide new evidence of neural drive regulation during shortening and lengthening muscle actions.

NEW & NOTEWORTHY Using ultrasound-transparent high-density surface EMG, we simultaneously measured motor unit discharge and tibialis anterior fascicle length during shortening and lengthening contractions. Discharge rate was linearly related to fascicle length changes during both contraction types. However, when considering the same level of fascicle shortening between contractions, discharge rates were systematically lower during lengthening, and neuromechanical delays were prolonged, consistent with length-dependent adjustments in contractile properties. These findings provide new evidence of neuromechanical coupling during anisometric contractions.

fascicle length; high-density surface electromyography; motor unit; shortening and lengthening contractions; ultrasound

Correspondence: E. Martinez-Valdes (e.a.martinezvaldes@bham.ac.uk).
Submitted 30 April 2026 / Revised 17 June 2026 / Accepted 13 July 2026

0022-3077/26 Copyright © 2026 The Authors. Licensed under Creative Commons Attribution CC-BY 4.0.
Published by the American Physiological Society.

Downloaded from journals.physiology.org/journal/jn (130.192.232.231) on October 30, 2026.

INTRODUCTION

How the central nervous system translates descending motor commands into precisely controlled musculotendinous dynamics during voluntary movement remains a fundamental question in motor control (1). During anisometric contractions, muscles produce force while changing length, creating a complex interplay between neural drive, fascicle mechanics, and tendon force transmission that cannot be fully characterized from isometric studies alone (2). A key aspect of this interplay is the neuromechanical delay (i.e., the latency between an estimate of the neural drive to muscle and the resulting force) (3), which reflects the latencies of excitation-contraction coupling and series-elastic force transmission. Such delays depend on muscle length, as shown in a previous study (4).

Capturing these relations in vivo has been challenging. Previous work has attempted to relate motor unit (MU) discharge behavior to fascicle dynamics during dynamic contractions using intramuscular electromyography combined with ultrasonography in separate sessions (5). However, intramuscular techniques sample only a small muscle region, can be performed in a very limited range of motion, and yield few MUs, limiting the ability to represent the full neural drive to muscles (6, 7). An alternative approach uses high-density surface electromyography electrodes transparent to ultrasound (HDsEMG-US), which enable simultaneous recording of multiple MU spike trains and fascicle length (FL) from the same region of interest (8, 9). Using this approach, we previously characterized the relations between the cumulative spike train (CST), FL, and torque during isometric contractions of the tibialis anterior (TA), showing that discharge rate modulation is closely related to changes in FL (10). However, whether these neuromechanical relations hold during anisometric contractions, and how the direction (i.e., shortening or lengthening) of FL change influences MU discharge behavior and signal transmission delays, remains unknown.

The scarcity of evidence on this topic stems partly from the challenges in tracking MU action potential shapes during anisometric contractions, which has only been addressed with recent advances in decomposition algorithms, and partly because concurrent measurement of FL and MU discharge from the same muscle region has only become possible with the development of HDsEMG-US electrodes (8, 9). Addressing this gap is important because lengthening contractions involve distinct mechanical properties, including enhanced force production attributed to passive structural elements (11), which may alter the relation between neural drive and force output. Clarifying these relations is a key step toward explaining how lengthening produces comparable or greater torque with similar or even lower neural drive than shortening, which is a hallmark of eccentric behavior (2). Furthermore, while Oliveira and Negro (12) showed that rate coding, rather than additional recruitment, governs MU control during dynamic contractions at increasing velocities, the concurrent relation between MU discharge behavior and fascicle mechanics was not examined. As a result, it remains unclear how the type of FL change influence MU-fascicle coupling and the associated signal transmission delays during submaximal constant-load anisometric contractions.

Therefore, the purpose of this study was to address this gap by extending our previous isometric findings and characterizing MU-FL interactions during shortening and lengthening contractions using HDsEMG-US electrodes. Our hypotheses were motivated by two physiological features of lengthening actions. First, muscle twitches are slower at longer lengths (13) and passive elements, such as titin add series compliance and force (11), which should delay the transmission of neural drive to fascicle motion and tendon force. Second, the greater force produced per unit of neural drive, together with the lower motoneuron excitability reported during lengthening actions (14), reduces the drive needed to sustain a given torque (12). We therefore hypothesized that, during lengthening relative to shortening muscle actions, neuromechanical delays would be prolonged and MU discharge rates reduced.

METHODS

Participants, Study Design, and Setting

Ten healthy, physically active, young males [mean age (SD): 29 (5) yr] volunteered for this observational cross-sectional study, which is reported following STROBE guidelines (15). Data were collected at the University of Queensland's School of Human Movement and Nutrition Sciences Biomechanics Laboratory.

Exclusion criteria included neuromuscular disorders, any history of lower limb pain, and age below 18 or above 35 yr. All procedures complied with the Declaration of Helsinki and were approved by the University of Queensland Ethics Committee (approval: 2019001675). Written informed consent was obtained from all participants prior to testing.

Experimental Protocol

Participants attended the laboratory for a single testing session. They were seated in a reclined position on an isokinetic dynamometer (Humac Norm, CSMi) with the knee flexed to 10°. Three maximum voluntary contractions (MVCs) of ankle dorsiflexion were performed at a long muscle-tendon length (~30° of plantarflexion). The anisometric protocol comprised an isometric phase at 30° of plantarflexion (5 s), a shortening phase (15 s, 2°/s) from 30° to 0° of plantarflexion, an isometric hold at 0° of plantarflexion (5 s), and a lengthening phase (15 s, 2°/s) returning to 30° of plantarflexion (total range of motion of 30°). Torque was maintained at the 25% of MVC achieved at long muscle-tendon length (~30° of plantarflexion). The slow angular velocity (2°/s) was selected to improve the stability of MU action potentials during dynamic conditions (16). This protocol was repeated three times per participant. Visual feedback of the torque signal was displayed on a monitor as a moving bar, with a horizontal target line set at 25% MVC. Participants were instructed to maintain the bar on the target line throughout the range of motion.

Data Acquisition

Surface EMG signals were recorded from the TA using a 32-channel HDsEMG-US electrode grid (8×4 electrodes, 1 mm diameter, 10 mm interelectrode distance; ReC Bioengineering and LISiN, Politecnico di Torino, Turin,

Downloaded from journals.physiology.org/journal/jn (130.192.232.231) on October 30, 2026.

Italy) (8). Monopolar signals were acquired at 2,048 Hz with 16-bit resolution using a wireless wearable amplifier (17) (gain: 192 ± 1 V/V; bandpass: 10–500 Hz) (MEACS, ReC Bioengineering and LISiN, Politecnico di Torino, Turin, Italy). B-mode ultrasound images were captured at 80 frames/s (6 MHz, 60 mm field of view) using a 128-element transducer (LF9-5N60-A3; Telemed, Lithuania) positioned over the HDsEMG-US grid, which was placed over the proximal portion of the TA. The frame-rate of the US device was controlled via an external trigger set at 80 Hz, which was synchronized with HDsEMG signals (Micro 1401-3; Cambridge Electronic Design, UK). A detailed description of the instrumentation and recording setup has been provided previously (10). The experimental setup is illustrated in Fig. 1.

Data Analysis

HDsEMG signals were decomposed into MU spike trains using a validated convolutive blind-source separation algorithm (18). The monopolar signals were extended (extension factor of 16) and the decomposition was run for up to 500 iterations per recording. MUs were accepted at a silhouette (SIL) threshold of ≥0.86, which is slightly lower than the standard 0.90 threshold to account for the reduced selectivity of HDsEMG-US grids. Each spike train was further examined manually by an experienced operator; firings separated from the next by <33.3 ms or >200 ms were rechecked and, where necessary, the MU pulse train was re-estimated (19, 20). Changes in muscle length across the range of motion, from 0° to 30° of plantarflexion, can alter muscle geometry and MUAP shape, thereby potentially reducing decomposition accuracy during dynamic contractions. Therefore, a slow angular velocity of 2°/s was used, and isometric phases were interposed within the movement to minimize these nonstationarities, consistent with previous dynamic decomposition studies (12, 16). To verify that the same MUs could be reliably identified across the range of motion, individual MUs were tracked between the two extreme joint positions, 0° and 30° of plantarflexion, by cross-correlating their two-dimensional MUAP representations. Two MUs were considered to represent the same MU when the cross-correlation coefficient exceeded 0.80 (21). A representative tracked MU showed minimal MUAP shape variation across the range of motion, with a cross-correlation coefficient of 0.89 (Fig. 2*B*), consistent with our previous HDsEMG-US work in the same muscle (10). The same cross-correlation criterion was also used to screen for duplicate MUs; however, because of the relatively low MU yield, no duplicate MUs were identified, and therefore no duplicate removal was required. FL was tracked from the superficial compartment of the muscle, between the superficial and central aponeuroses, using the Lucas–Kanade optical flow algorithm with affine transformation (22). Individual MU discharge times were summed to generate a CST (23). The CST represents the combined discharge activity of the identified MUs. Because summation largely cancels their independent inputs, it provides an estimate of the common synaptic input, or neural drive, to the muscle, which is closely related to the resulting force output (24). The CST, FL, and torque signals were bandpass filtered (0.75–2 Hz, 4th order zero-phase Butterworth) and cross-correlated independently during the shortening and lengthening phases to assess associations and neuromechanical delays. For MUs active throughout both phases, linear regression was used to assess the rate of change in discharge rate per unit change in FL (i.e., delta discharge rate vs. delta FL) across 20 equally spaced epochs (10 per contraction phase; each epoch spanned 3° of ankle rotation, corresponding to ~1.5 s at 2°/s), thereby quantifying how much discharge rate changed for a given change in fascicle shortening or lengthening. Delta FL was calculated for each epoch as the change in FL relative to the longest length at the start of the shortening phase (30° of plantarflexion).

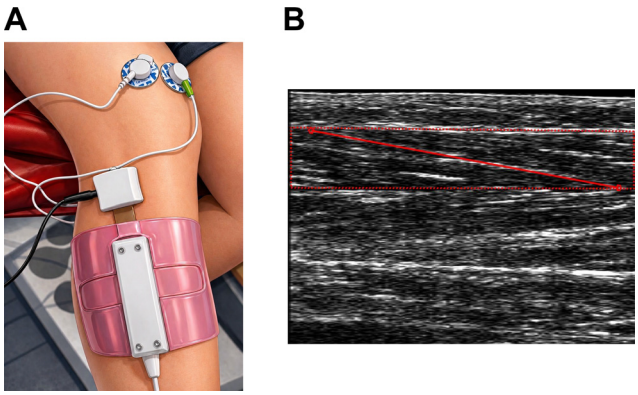


Figure 1. Experimental setup for simultaneous HDsEMG-US recordings. *A*: the 32-channel HDsEMG-US electrode grid (transparent, pink) was positioned over the proximal portion of the tibialis anterior, with the B-mode ultrasound transducer (white) placed directly over the electrode. The wireless wearable EMG amplifier (small white unit) was secured proximal to the electrode. Reference electrodes were placed over the patella. *B*: representative B-mode ultrasound image acquired through the HDsEMG-US electrode, showing the superficial and central aponeuroses of the tibialis anterior with a tracked fascicle segment (red line). Fascicle length was measured from the superficial compartment using the Lucas–Kanade optical flow algorithm. This configuration enabled concurrent recording of motor unit spike trains and fascicle length changes from the same muscle region during anisometric contractions. The experimental setup and ultrasound image are representative examples from one participant ($n = 1$).

Statistical Analysis

Statistical analyses were performed using mixed-effects models fitted with restricted maximum likelihood (REML) estimation (GraphPad Prism, v. 11.0.0; GraphPad Software, San Diego, CA). Results are expressed as means and standard deviations. Participant was included as a random factor in all models to account for the nonindependence of observations arising from multiple MUs nested within the same individual and repeated measures across epochs, as MU discharge rates are correlated within individuals (25, 26). Cross-correlation coefficients and delays were analyzed with contraction phase (shortening, lengthening) and signal comparison (CST vs. torque, CST vs. FL, FL vs. torque) as fixed factors. Discharge rate and FL were analyzed across the range of motion, divided into 10 epochs at 3° increments per contraction phase (30° to 3° during shortening, 3° to 30° during lengthening; 20 epochs total), with angular position and variable (FL, discharge rate) as fixed factors. Tukey's post hoc comparisons identified at which angular positions discharge rate differed between shortening and lengthening. Simple linear regression was used to assess the rate of change in discharge rate per unit change in FL (i.e., delta

Downloaded from journals.physiology.org/journal/jn (130.192.232.231) on October 30, 2026.

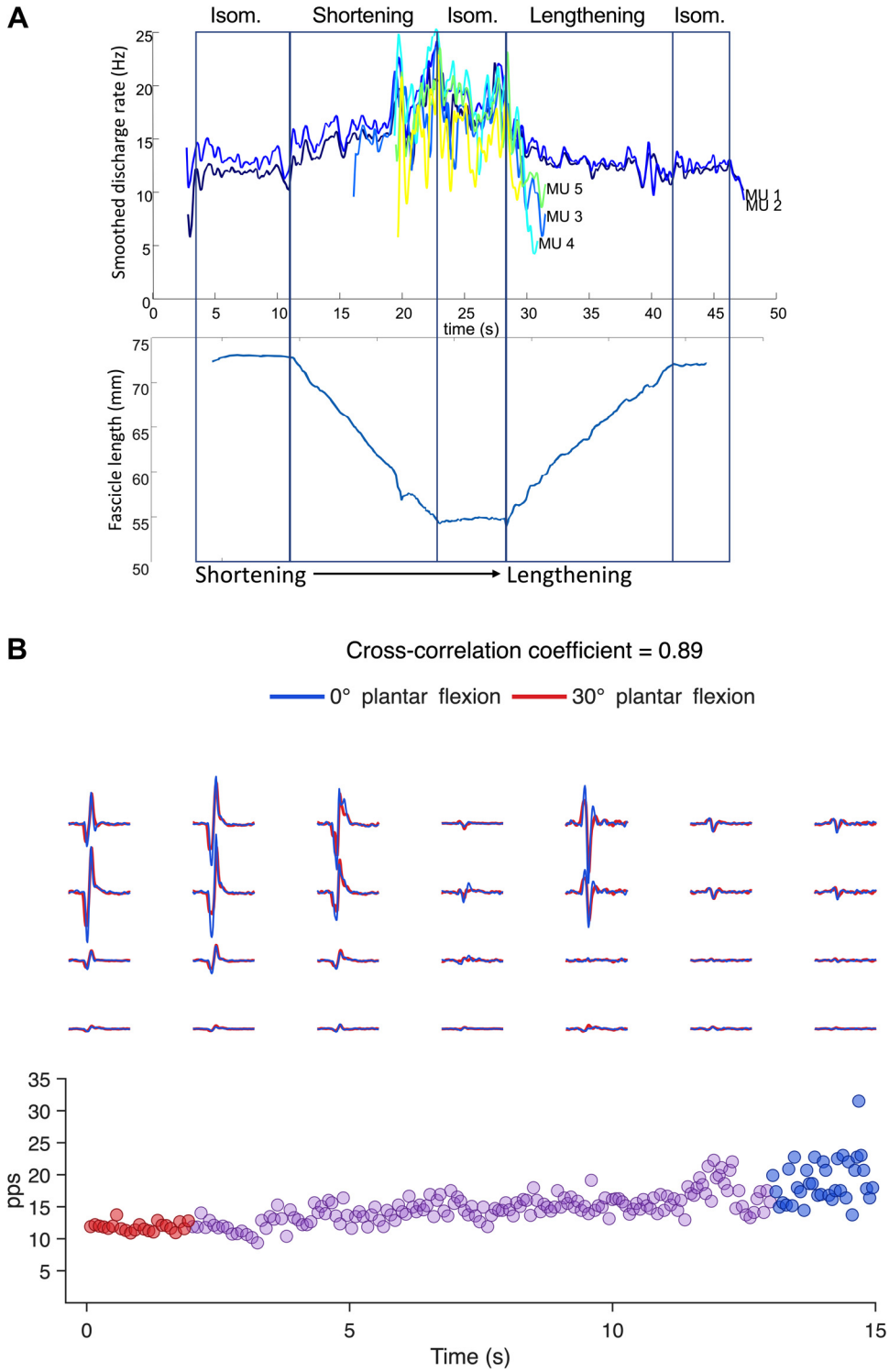


Figure 2. Motor unit discharge rates and tracking during anisometric contractions. *A*: a representative example from one participant ($n = 1$) showing five motor units identified during shortening and lengthening contractions at a speed of 2°/s, at a fixed torque level (25% MVC obtained at 30° of plantarflexion). Motor unit firing times were smoothed (2 Hz low-pass filter) to appreciate common fluctuations in firing rate between units (*top*). Changes in fascicle length can be appreciated on the bottom of the figure. *B*: motor unit tracking during the shortening phase. A representative example of a motor unit tracked across the range of motion during shortening can be seen in the figure ($n = 1$ participant). Each waveform corresponds to one single-differential EMG channel, and the action potentials belonging to this unit can be seen spread across the 28 EMG channels of the grid. The motor unit action potentials extracted at the two extremes of the movement, at the start of the contraction, when the muscle was at its longest length (red, 30° plantarflexion), and at the most shortened position, where discharge rate peaked (blue, 0° plantarflexion), were matched by cross-correlation as described previously (21), yielding a cross-correlation coefficient of 0.89. The instantaneous firing rate of this unit during the first half of the shortening phase can be seen at the bottom of the figure.

discharge rate vs. delta FL) for MUs continuously active during both phases, across 20 equally spaced epochs, thereby quantifying how much discharge rate changed for a given change in fascicle shortening or lengthening; slopes and intercepts were compared between contraction phases. Statistical significance was set at $P < 0.05$. Effect sizes are reported as mean differences with 95% confidence intervals and coefficients of determination (R^2).

RESULTS

MU Decomposition

MUs were accurately identified [SIL: 0.87 (0.01)] in eight of the 10 participants for at least 80% of the duration of both the shortening and lengthening phases, yielding an average of 4 ± 1 MUs per participant (per-participant yields are provided in Supplemental Table S1). However, in only five of the

Downloaded from journals.physiology.org/journal/jn (130.192.232.231) on October 30, 2026.

10 participants could MUs be tracked for the full duration of both contraction phases, with an average of 2 ± 1 MUs per participant. An example of the smoothed firing rate of five MUs identified during shortening and lengthening contractions is shown in Fig. 2*A*. In this example, and across all identified MUs, discharge rates were consistently lower during the lengthening phase compared with the shortening phase.

Decomposition accuracy across the range of motion was assessed by comparing the MUAP shape of tracked units between the two extremes of the movement. To depict this, a representative tracked unit during the shortening phase is shown in Fig. 2*B*, with minimal change in MUAP shape between 30° and 0° of plantarflexion (cross-correlation coefficient = 0.89), confirming reliable MU identification during these constant-load anisometric contractions.

Fascicle Length, Torque, and MU Discharge Rate Relations

High cross-correlation coefficients were obtained for all signal comparisons during both contraction phases. The common fluctuations of the three signals during the shortening and lengthening phases are illustrated for a representative participant in Fig. 3*A*. Group mean cross-correlation coefficients (min–max range) across all eight participants were as follows: during shortening, 0.68 (0.46–0.80) for CST versus torque, 0.63 (0.44–0.81) for CST versus FL, and 0.85 (0.76–0.96) for torque versus FL; during lengthening, values were 0.68 (0.52–0.85), 0.62 (0.48–0.81), and 0.87 (0.75–0.94), respectively.

The correlation between FL and torque was significantly higher than both CST versus torque and CST versus FL (signal comparison effect: $F_{2,14} = 33.6$, $P < 0.0001$; Fig. 3*B*). Cross-correlation delays were significantly longer during the lengthening phase compared with the shortening phase (phase effect: $F_{1,7} = 8.51$, $P = 0.023$; mean difference: −25.04 ms, 95% CI: −45.35 to −4.74; Fig. 3*C*).

For the five participants in whom MUs were tracked for the full duration of both contraction phases, discharge rate decreased as FL increased during both shortening and lengthening (Fig. 4*A*). All tracked MUs reduced their discharge rate during the lengthening phase despite showing no changes in FL when comparing similar joint-position instants between contraction phases. Linear regression confirmed a significant positive relation between delta FL and discharge rate during both shortening ($R^2 = 0.43$, $F_{1,57} = 43.62$, $P < 0.0001$; Fig. 4*B*) and lengthening ($R^2 = 0.35$, $F_{1,53} = 28.10$, $P < 0.0001$; Fig. 4*B*), with this relation being consistent at the individual participant level (Fig. 4, *C* and *D*). The slopes did not differ between contraction phases ($F_{1,110} = 0.60$, $P = 0.44$; pooled slope: 0.25), but the intercepts were significantly different ($F_{1,111} = 116.7$, $P < 0.0001$; Fig. 4*B*). This indicated that during lengthening, discharge rate was systematically lower across the range of motion, such that for any given change in FL, discharge rate was consistently lower during lengthening than during shortening.

DISCUSSION

This study used HDsEMG-US electrodes to characterize MU discharge behavior and TA fascicle dynamics during shortening and lengthening contractions, yielding three key findings. First, strong cross-correlations between CST, FL, and torque persisted across both phases, supporting the use of the approach for dynamic contractions. Second, neuromechanical delays were longer during the lengthening phase. Finally, MU discharge rates remained consistently lower during lengthening, despite similar FL trajectories and discharge rate-FL slopes.

The high cross-correlation coefficients between CST, FL, and torque during both phases confirm that the HDsEMG-US approach captures meaningful neuromechanical relations under dynamic conditions, extending the isometric validation (10) to contractions in which MU action potential waveforms are less stable. The finding that FL-torque correlations exceeded CST-torque and CST-FL correlations is expected, given that torque is a more direct mechanical consequence of fascicle shortening than of neural discharge patterns.

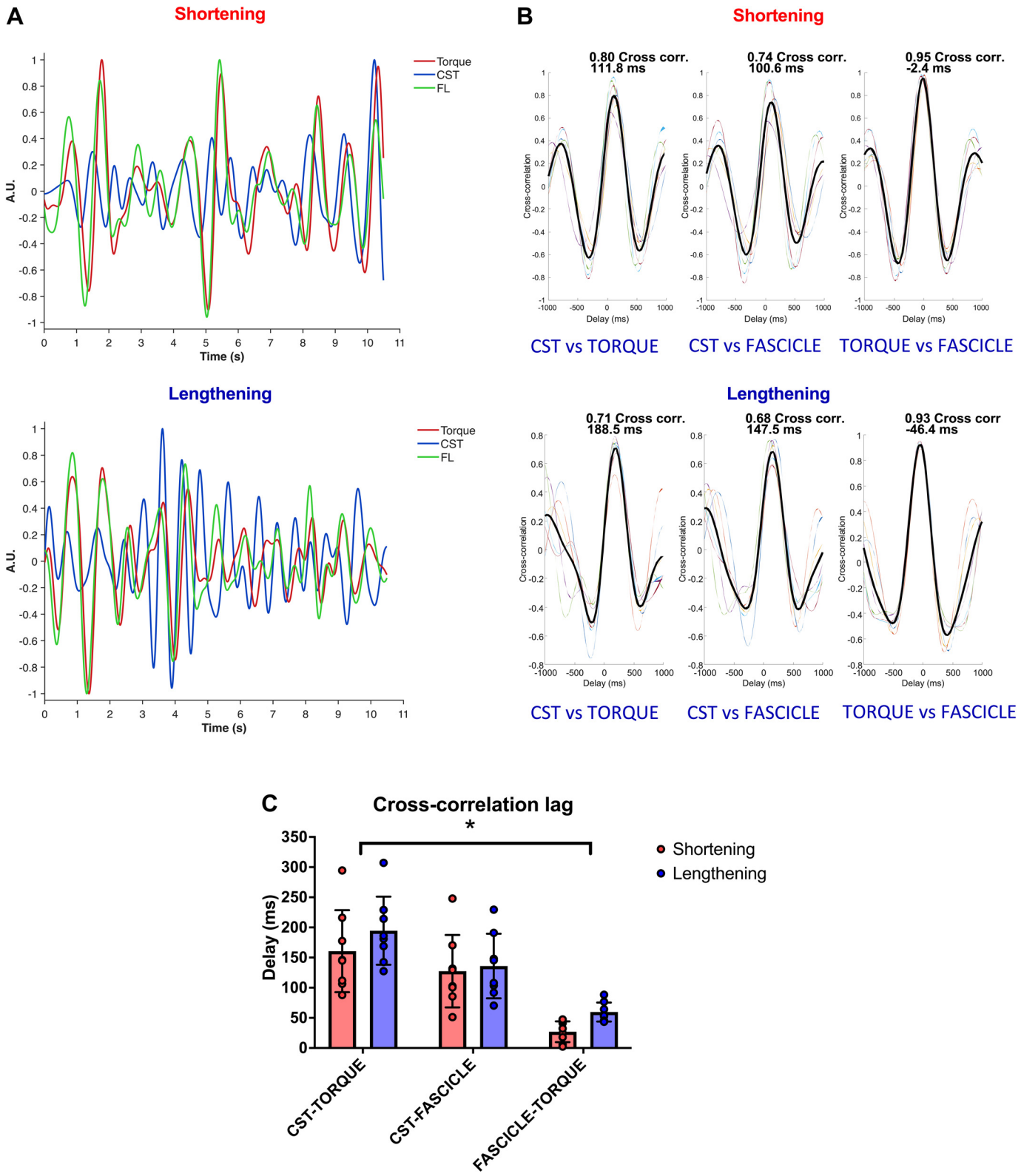
The prolonged neuromechanical delays during lengthening are consistent with our isometric findings at longer muscle lengths (10) and demonstrate that this phenomenon persists under dynamic conditions, aligning with foundational evidence that electromechanical delays are inherently modulated by contraction type (4). Marsh et al. (13) observed that when the TA was positioned at greater lengths, muscle twitches were larger with increased contraction time and half-relaxation time, and that torque produced at longer lengths was higher than at shorter lengths when stimulated at rates comparable to those in our study (10–20 Hz). Considering that mean discharge rate was similar across joint angles at relative torque targets during isometric contractions (10), it is likely that slower twitches at longer FLs delayed both muscle contraction and force transmission to the tendon. Similar mechanisms could explain the prolonged delays during lengthening, as a lower discharge rate was required to maintain the same torque level as during shortening. In addition, passive structural elements, such as titin may contribute to force enhancement during lengthening contractions and, given its spring-like behavior (11, 27), these elements could further increase the lag between neural drive and tendon force. Together, these contractile and passive mechanisms likely contribute to the prolonged neuromechanical delays observed during lengthening.

A potential alternative explanation is that the longer delays during lengthening arise from the torque-generation characteristics of the isokinetic dynamometer, for example, if the servomotor responded differently between the lengthening and shortening phases. Although this possibility cannot be entirely excluded for the delays involving torque, it is unlikely to account for our findings. Importantly, the phase-dependent increase in delay was also present in the CST-FL comparison, which is derived solely from the neural drive (HDsEMG) and FL changes (ultrasound) and is therefore independent of the dynamometer motor. Together with the very low, matched angular velocity (2°/s) and the feedback-matched torque between phases, this indicates that the prolonged lengthening delay reflects a genuine neuromechanical phenomenon rather than a dynamometer artifact.

The phase-dependent differences across all three delays may also reflect a contraction-type-specific, nonlinear transformation of MU action activity to torque. Because

Downloaded from journals.physiology.org/journal/jn (130.192.232.231) on October 30, 2026.

mechanically coupled muscle fibers share a common compliance, their forces sum nonadditively (28), and the extent of this nonlinearity depends on the mechanical state of the muscle, which differs between shortening and lengthening. Although this nonadditive summation has been characterized mainly under isometric conditions and for force magnitude, the available evidence suggests that it is altered by movement; summation nonlinearities



Downloaded from journals.physiology.org/journal/jn (130.192.232.231) on October 30, 2026.

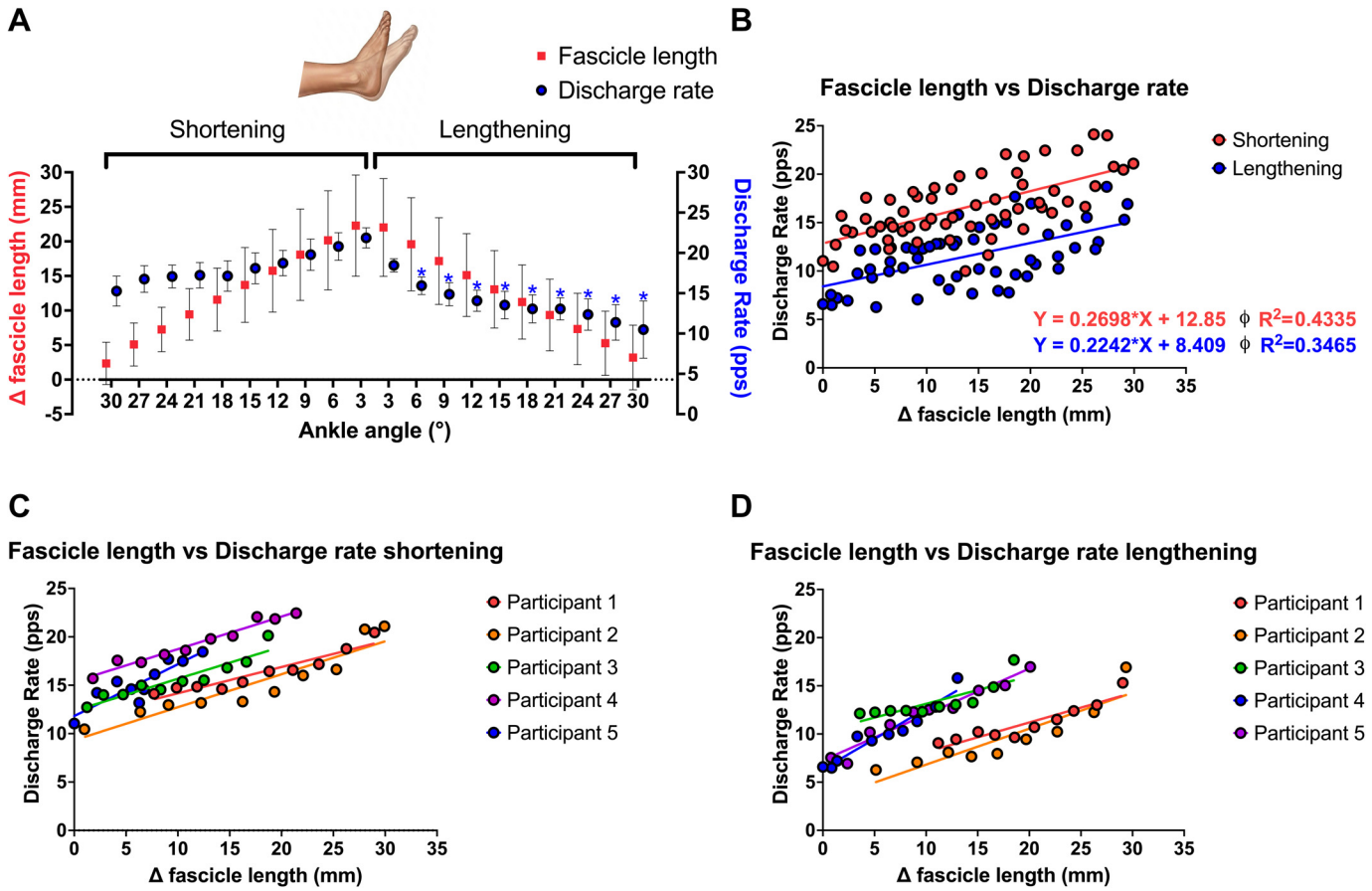


Figure 4. Fascicle length changes (delta fascicle length) and discharge rate relations during anisometric contractions. Data in all panels were obtained from five participants ($n = 5$). *A*: changes in fascicle length and discharge rate during shortening and lengthening phases of the contraction. *B*: linear relations between changes in fascicle length and discharge rate during shortening (red regression line) and lengthening (blue regression line) phases of the contractions based on population-level results. *C*: linear relations between changes in fascicle length and discharge rate during shortening for individual participants, where each line is one participant's regression, and each point is that participant's mean discharge rate and mean delta fascicle length within an epoch. *D*: the same linear relations during lengthening for individual participants. *Significant differences in discharge rate between shortening and lengthening at the same joint angle ($P < 0.05$). ΦSignificant differences between regression intercepts ($P < 0.05$).

decrease during shortening (29), and slow shortening can even increase the force of small MUs (30), likely because movement reduces the viscoelastic coupling between fibers, leaving the common tendon as the dominant source of coupling. Such movement- and direction-dependent changes in the action potential-to-torque transformation could therefore contribute to the different delays observed between shortening and lengthening. As these effects have so far been described almost exclusively in reduced animal preparations, the present approach offers a means to probe such neural-to-mechanical transformations noninvasively in vivo in humans.

Although the neural-to-mechanical transformation is likely nonlinear and contraction-type dependent, the relatively narrow range of motion used in the present study may have constrained the system to an approximately linear portion of the torque-length relation. Moreover, opposing nonlinear contributions from active and passive force components may have partially compensated for one another, thereby linearizing the neural drive required to maintain the target torque across this working range. This interpretation is consistent with the parallel DR-FL slopes observed in both contraction phases. In this context, the intercept shift between contraction types likely

Figure 3. Signal relations and cross-correlation lag (delay) results during anisometric contractions. *A*: common fluctuations from the three generated signals, torque (red), CST (blue), and fascicle length (FL, green), during the shortening (*top*) and lengthening (*bottom*) phases in a representative participant ($n = 1$); each signal was bandpass-filtered (0.75–2 Hz) and normalized to its peak (maximum absolute) amplitude (arbitrary units, A.U.). *B*: cross-correlation (CC) and lag results between cumulative spike train (CST) versus torque, CST versus fascicle length (fascicle), and fascicle versus torque from a single representative participant ($n = 1$) during shortening (*B*, *top*) and lengthening (*B*, *bottom*) phases of the contractions. For each pair, the lag indicates the time by which the first-named signal leads the second; a positive value therefore means the first signal precedes the second, whereas a negative value means it follows it. Accordingly, the positive CST versus torque and CST versus fascicle lags indicate that neural drive (CST) precedes both fascicle-length changes and torque, while the negative torque versus fascicle lags (−2.4 ms and −46.4 ms) indicate that fascicle-length changes precede torque, consistent with the expected physiological sequence in which neural drive leads to fascicle shortening, which in turn produces torque. *C*: group cross-correlation lag results ($n = 8$ participants) during shortening (red) and lengthening (blue) phases of the contraction, expressed as the magnitude of the delay between each signal pair (means ± SD with individual data points). *Significant effect of contraction type (lengthening vs. shortening, $P < 0.05$).

Downloaded from journals.physiology.org/journal/jn (130.192.232.231) on October 30, 2026.

reflects the reduced motoneuron pool excitation needed during lengthening, where the enhanced mechanical output per discharge, from both the contractile potentiation and passive force contributions described above, would permit the same torque to be maintained with less neural drive.

The systematic reduction in discharge rate during lengthening, despite parallel discharge rate-FL regression slopes, aligns well with previous findings. Pasquet et al. (5) reported higher shortening than lengthening discharge rates in the TA, Oliveira and Negro (12) demonstrated consistently higher shortening than lengthening discharge rates across multiple velocities (5–20°/s) during constant-load contractions in the same muscle, suggesting that this pattern may persist beyond the slow velocity tested here, and Søgaard et al. (31) observed a similar pattern in the brachial biceps. The present study extends these observations by simultaneously measuring FL and MU discharge from the same muscle region, revealing that this contraction-type difference manifests as an intercept shift in the DR-FL relation rather than a change in slope. The small differences in the rate of DR modulation with FL reported by Oliveira and Negro (12) likely reflect the use of joint angle as a surrogate for muscle length and the higher contraction velocities used (5–20°/s vs. 2°/s). The lower discharge rate during lengthening is consistent with enhanced force per unit of neural drive during lengthening contractions. Specifically, as described above, the enhanced contractile (13) and passive force contributions (11) during lengthening reduce the neural input required to sustain the target torque at any given joint angle. Furthermore, as rate coding rather than additional recruitment governs MU control during dynamic contractions (12), the modulation observed here likely reflects firing rate adjustments rather than changes in the active MU pool. The parallel regression slopes suggest that MU discharge sensitivity to FL changes is preserved regardless of contraction type, with the lower lengthening discharge rates representing a global reduction in excitatory drive to the motoneuron pool, as muscle length changes may directly influence shared synaptic inputs to spinal motor neurons (32). This is consistent with the reduced corticospinal excitability and increased presynaptic inhibition of Ia afferents reported during eccentric contractions (14), which together lower the net excitatory input to the motoneuron pool while the enhanced passive and contractile force contributions compensate for this reduced neural drive.

An important methodological consideration when interpreting the discharge rate findings is that torque was maintained at 25% of MVC measured at a long muscle-tendon length (~30° of plantarflexion), rather than at angle-specific MVCs. Because the TA's force-generating capacity varies with joint angle, the participant's relative effort changed across the range of motion. Accordingly, the discharge rates reported here reflect not muscle length per se but the relative force demand imposed by the muscle length-dependent force-generating capacity. For example, at more shortened positions (near 0° of plantarflexion), the muscle operates further from its force-length optimum, and therefore a greater proportion of its maximal capacity (and consequently a higher discharge rate) is needed to produce the same absolute torque (Fig. 2*B*). Conversely, at lengthened positions closer to the optimum, the same torque requires proportionally less effort and lower discharge rates. This interpretation is supported by Cudicio et al. (33), who showed that when torque targets are set relative to angle-specific MVCs, matched MU discharge rates remain similar across muscle lengths, with the differences in force-generation capacity being explained by MU twitch properties rather than discharge rate modulation. In the present study, the use of a single reference MVC likely amplified the observed differences in discharge rate across the range of motion, particularly at the extremes. Future studies should consider angle-specific torque normalization to separate the contributions of neural drive modulation from those imposed by the force-length relation.

Several limitations should be acknowledged. The lower MU yield (4 ± 1 per participant) likely due to the 32-channel configuration, which has fewer electrodes and a larger interelectrode distance (10 mm) than other denser configurations often used in decomposition studies (34). In addition, the flexibility of the electrode may have caused subtle variations in interelectrode distance, potentially compromising MUAP stability during dynamic contractions. Only five participants provided continuous MU tracking across both phases, as MU action potential waveforms can change shape during dynamic contractions due to relative movement between the electrode and muscle fibers, making it difficult to track the same MU throughout the full range of motion. This limited the statistical power of the regression analysis. Nevertheless, the effect size was large enough to yield consistent results across these participants, as evidenced by the uniform direction of the DR-FL relations observed individually (Fig. 4, *C* and *D*). The use of a single muscle (TA) and a slow angular velocity (2°/s) constrains generalization to other muscles, contraction speeds, and torque levels. Faster contraction velocities increase the rate of change in MU action potential waveforms, making continuous MU tracking across the full range of motion more challenging and reducing decomposition accuracy. In addition, the task involved constant-load lengthening contractions rather than true eccentric contractions, in which the external load exceeds the torque produced at the joint. Although this constant-load paradigm facilitates reliable MU decomposition, it does not reproduce the mechanics of eccentric overload, and the imposed constant torque also differs from real-world dynamic movements, in which torque varies with joint angle. These factors constrain the extent to which our findings generalize to natural and to true eccentric muscle actions. Despite these constraints, the consistent findings support the robustness of the observed neuromechanical relations. In future studies, advances in decomposition techniques and electrode design should significantly improve MU yield. These improvements will facilitate the simultaneous assessment of FL and MU activity during anisometric contractions across more challenging motor tasks and diverse populations, such as older individuals, further elucidating how contraction speed and torque characteristics modulate neural drive.

Conclusions

This study demonstrates that HDsEMG-US electrodes can characterize MU-fascicle interactions during anisometric contractions. Neuromechanical delays were prolonged, and

Downloaded from journals.physiology.org/journal/jn (130.192.232.231) on October 30, 2026.

MU discharge rates were reduced during lengthening relative to shortening, despite similar FL trajectories and discharge rate-FL slopes. These findings extend our understanding of neuromechanical coupling during dynamic muscle actions and highlight the potential of HDsEMG-US for studying neuromechanical interactions during functional conditions.

DATA AVAILABILITY

Data will be made available upon reasonable request.

SUPPLEMENTAL MATERIAL

Supplemental Table S1: https://doi.org/10.6084/m9.figshare.32706741.

GRANTS

This study was partially funded by the University of Birmingham International Engagement Fund (BIEF) (awarded to E.M.-V.).

DISCLOSURES

No conflicts of interest, financial or otherwise, are declared by the authors.

AUTHOR CONTRIBUTIONS

P.A.P. and E.M.-V. conceived and designed research; P.A.P. and E.M.-V. performed experiments; M.A. and E.M.-V. analyzed data; M.A., P.A.P., F.N., A.B., G.L.C., and E.M.-V. interpreted results of experiments; M.A. and E.M.-V. prepared figures; M.A. drafted manuscript; M.A., P.A.P., F.N., A.B., G.L.C., and E.M.-V. edited and revised manuscript; M.A., P.A.P., F.N., A.B., G.L.C., and E.M.-V. approved final version of manuscript.

REFERENCES

1. **Enoka RM.** Biomechanics and neuroscience: a failure to communicate. *Exerc Sport Sci Rev* 32: 1–3, 2004. doi:10.1097/00003677-200401000-00001.
2. **Duchateau J**, **Enoka RM.** Neural control of lengthening contractions. *J Exp Biol* 219: 197–204, 2016. doi:10.1242/jeb.123158.
3. **Del Vecchio A**, **Úbeda A**, **Sartori M**, **Azorín JM**, **Felici F**, **Farina D.** Central nervous system modulates the neuromechanical delay in a broad range for the control of muscle force. *J Appl Physiol (1985)* 125: 1404–1410, 2018. doi:10.1152/japplphysiol.00135.2018.
4. **Cavanagh PR**, **Komi PV.** Electromechanical delay in human skeletal muscle under concentric and eccentric contractions. *Eur J Appl Physiol Occup Physiol* 42: 159–163, 1979. doi:10.1007/BF00431022.
5. **Pasquet B**, **Carpentier A**, **Duchateau J.** Specific modulation of motor unit discharge for a similar change in fascicle length during shortening and lengthening contractions in humans. *J Physiol* 577: 753–765, 2006. doi:10.1113/jphysiol.2006.117986.
6. **Farina D**, **Merletti R**, **Enoka RM.** The extraction of neural strategies from the surface EMG: 2004-2024. *J Appl Physiol (1985)* 138: 121–135, 2025. doi:10.1152/japplphysiol.00453.2024.
7. **Farina D**, **Negro F**, **Muceli S**, **Enoka RM.** Principles of motor unit physiology evolve with advances in technology. *Physiology (Bethesda)* 31: 83–94, 2016. doi:10.1152/physiol.00040.2015.
8. **Botter A**, **Vieira TM**, **Loram ID**, **Merletti R**, **Hodson-Tole EF.** A novel system of electrodes transparent to ultrasound for simultaneous detection of myoelectric activity and B-mode ultrasound images of skeletal muscles. *J Appl Physiol (1985)* 115: 1203–1214, 2013. doi:10.1152/japplphysiol.00090.2013.
9. **Cerone GL**, **Vieira T**, **Gazzoni M**, **Botter A.** ReGrid: a highly conformable and ultrasound transparent patch for HD-sEMG detection. *IEEE Trans Neural Syst Rehabil Eng* 34: 1048–1059, 2026. doi:10.1109/TNSRE.2026.3663330.
10. **Martinez-Valdes E**, **Negro F**, **Botter A**, **Pincheira PA**, **Cerone GL**, **Falla D**, **Lichtwark GA**, **Cresswell AG.** Modulations in motor unit discharge are related to changes in fascicle length during isometric contractions. *J Appl Physiol (1985)* 133: 1136–1148, 2022. doi:10.1152/japplphysiol.00758.2021.
11. **Herzog W.** Mechanisms of enhanced force production in lengthening (eccentric) muscle contractions. *J Appl Physiol (1985)* 116: 1407–1417, 2014. doi:10.1152/japplphysiol.00069.2013.
12. **Oliveira AS**, **Negro F.** Neural control of matched motor units during muscle shortening and lengthening at increasing velocities. *J Appl Physiol (1985)* 130: 1798–1813, 2021. doi:10.1152/japplphysiol.00043.2021.
13. **Marsh E**, **Sale D**, **McComas AJ**, **Quinlan J.** Influence of joint position on ankle dorsiflexion in humans. *J Appl Physiol Respir Environ Exerc Physiol* 51: 160–167, 1981. doi:10.1152/jappl.1981.51.1.160.
14. **Duchateau J**, **Baudry S.** Insights into the neural control of eccentric contractions. *J Appl Physiol (1985)* 116: 1418–1425, 2014. doi:10.1152/japplphysiol.00002.2013.
15. **von Elm E**, **Altman DG**, **Egger M**, **Pocock SJ**, **Gøtzsche PC**, **Vandenbroucke JP**; **STROBE Initiative.** Strengthening the Reporting of Observational Studies in Epidemiology (STROBE) statement: guidelines for reporting observational studies. *Bmj* 335: 806–808, 2007. doi:10.1136/bmj.39335.541782.AD.
16. **Glaser V**, **Holobar A.** Motor unit identification from high-density surface electromyograms in repeated dynamic muscle contractions. *IEEE Trans Neural Syst Rehabil Eng* 27: 66–75, 2019. doi:10.1109/TNSRE.2018.2885283.
17. **Cerone GL**, **Botter A**, **Gazzoni M.** A modular, smart, and wearable system for high density sEMG detection. *IEEE Trans Biomed Eng* 66: 3371–3380, 2019. doi:10.1109/TBME.2019.2904398.
18. **Negro F**, **Muceli S**, **Castronovo AM**, **Holobar A**, **Farina D.** Multi-channel intramuscular and surface EMG decomposition by convolutive blind source separation. *J Neural Eng* 13: 026027, 2016. doi:10.1088/1741-2560/13/2/026027.
19. **Afsharipour B**, **Manzur N**, **Duchcherer J**, **Fenrich KF**, **Thompson CK**, **Negro F**, **Quinlan KA**, **Bennett DJ**, **Gorassini MA.** Estimation of self-sustained activity produced by persistent inward currents using firing rate profiles of multiple motor units in humans. *J Neurophysiol* 124: 63–85, 2020. doi:10.1152/jn.00194.2020.
20. **Boccia G**, **Martinez-Valdes E**, **Negro F**, **Rainoldi A**, **Falla D.** Motor unit discharge rate and the estimated synaptic input to the vasti muscles is higher in open compared with closed kinetic chain exercise. *J Appl Physiol (1985)* 127: 950–958, 2019. doi:10.1152/japplphysiol.00310.2019.
21. **Martinez-Valdes E**, **Negro F**, **Laine CM**, **Falla D**, **Mayer F**, **Farina D.** Tracking motor units longitudinally across experimental sessions with high-density surface electromyography. *J Physiol* 595: 1479–1496, 2017. doi:10.1113/JP273662.
22. **Farris DJ**, **Lichtwark GA.** UltraTrack: Software for semi-automated tracking of muscle fascicles in sequences of B-mode ultrasound images. *Comput Methods Programs Biomed* 128: 111–118, 2016. doi:10.1016/j.cmpb.2016.02.016.
23. **Thompson CK**, **Negro F**, **Johnson MD**, **Holmes MR**, **McPherson LM**, **Powers RK**, **Farina D**, **Heckman CJ.** Robust and accurate decoding of motoneuron behaviour and prediction of the resulting force output. *J Physiol* 596: 2643–2659, 2018. doi:10.1113/JP276153.
24. **Farina D**, **Negro F**, **Dideriksen JL.** The effective neural drive to muscles is the common synaptic input to motor neurons. *J Physiol* 592: 3427–3441, 2014. doi:10.1113/jphysiol.2014.273581.
25. **Arvanitidis M**, **Falla D**, **Negro F**, **Boccia G**, **Rainoldi A**, **Martinez-Valdes E.** Reduced knee extensor torque steadiness and increased motor unit discharge rate variability in young people with patellofemoral pain: a pilot study. *Eur J Appl Physiol* 126: 2595–2615, 2026. doi:10.1007/s00421-025-06083-8.
26. **Tenan MS**, **Marti CN**, **Griffin L.** Motor unit discharge rate is correlated within individuals: a case for multilevel model statistical analysis. *J Electromyogr Kinesiol* 24: 917–922, 2014. doi:10.1016/j.jelekin.2014.08.014.
27. **Nishikawa KC**, **Monroy JA**, **Uyeno TE**, **Yeo SH**, **Pai DK**, **Lindstedt SL.** Is titin a 'winding filament'? A new twist on muscle contraction. *Proc Biol Sci* 279: 981–990, 2012. doi:10.1098/rspb.2011.1304.
28. **Perreault EJ**, **Day SJ**, **Hulliger M**, **Heckman CJ**, **Sandercock TG.** Summation of forces from multiple motor units in the cat soleus muscle. *J Neurophysiol* 89: 738–744, 2003. doi:10.1152/jn.00168.2002.

Downloaded from journals.physiology.org/journal/jn (130.192.232.231) on October 30, 2026.

29. **Powers RK**, **Binder MD.** Summation of motor unit tensions in the tibialis posterior muscle of the cat under isometric and nonisometric conditions. *J Neurophysiol* 66: 1838–1846, 1991. doi:10.1152/jn.1991.66.6.1838.
30. **Heckman CJ**, **Weytjens JL**, **Loeb GE.** Effect of velocity and mechanical history on the forces of motor units in the cat medial gastrocnemius muscle. *J Neurophysiol* 68: 1503–1515, 1992. doi:10.1152/jn.1992.68.5.1503.
31. **Søgaard K**, **Christensen H**, **Jensen BR**, **Finsen L**, **Sjøgaard G.** Motor control and kinetics during low level concentric and eccentric contractions in man. *Electroencephalogr Clin Neurophysiol* 101: 453–460, 1996.
32. **Cabral HV**, **Inglis JG**, **Cudicio A**, **Cogliati M**, **Orizio C**, **Yavuz US**, **Negro F.** Muscle contractile properties directly influence shared synaptic inputs to spinal motor neurons. *J Physiol* 602: 2855–2872, 2024. doi:10.1113/JP286078.
33. **Cudicio A**, **Martinez-Valdes E**, **Cogliati M**, **Orizio C**, **Negro F.** The force-generation capacity of the tibialis anterior muscle at different muscle-tendon lengths depends on its motor unit contractile properties. *Eur J Appl Physiol* 122: 317–330, 2022. doi:10.1007/s00421-021-04829-8.
34. **Martinez-Valdes E**, **Negro F**, **Farina D**, **Falla D.** Divergent response of low- versus high-threshold motor units to experimental muscle pain. *J Physiol* 598: 2093–2108, 2020. doi:10.1113/JP279225.

Downloaded from journals.physiology.org/journal/jn (130.192.232.231) on October 30, 2026.